AGU PUBLICATIONS

Geophysical Research Letters

RESEARCH LETTER
10.1002/2015GL063999

Key Points:
- Direct measurements of magnetic force acting on BBF plasma
- BBF plasma is accelerated toward Earth until it reaches 15 R_E, then braked
- Knowledge of the forces on BBFs provides clue to their fate close to Earth

Correspondence to:
T. Karlsson,
tomas.karlsson@ee.kth.se

Citation:
Karlsson, T., M. Hamrin, H. Nilsson, A. Kullen, and T. Pitkänen (2015), Magnetic forces associated with bursty bulk flows in Earth's magnetotail, *Geophys. Res. Lett.*, *42*, 3122–3128, doi:10.1002/2015GL063999.

Received 25 MAR 2015
Accepted 11 APR 2015
Accepted article online 15 APR 2015
Published online 7 MAY 2015

Magnetic forces associated with bursty bulk flows in Earth's magnetotail

Tomas Karlsson[1], Maria Hamrin[2], Hans Nilsson[3], Anita Kullen[1], and Timo Pitkänen[2]

[1]Space and Plasma Physics, School of Electrical Engineering, Royal Institute of Technology, Stockholm, Sweden, [2]Department of Physics, Umeå University, Umeå, Sweden, [3]Swedish Institute of Space Physics, Kiruna, Sweden

Abstract We present the first direct measurements of magnetic forces acting on bursty bulk flow plasma in the magnetotail. The magnetic forces are determined using Cluster multispacecraft measurements. We analyze 67 bursty bulk flow (BBF) events and show that the curvature part of the magnetic force is consistently positive, acting to accelerate the plasma toward Earth between approximately 10 and 20 R_E geocentrical distances, while the magnetic field pressure gradient increasingly brakes the plasma as it moves toward Earth. The net result is that the magnetic force accelerates the plasma at distances greater than approximately 14 R_E, while it acts to decelerate it within that distance. The magnetic force, together with the thermal pressure gradient force, will determine the dynamics of the BBFs as they propagate toward the near-Earth tail region. The determination of the former provides an important clue to the ultimate fate of BBFs in the inner magnetosphere.

1. Introduction

During the last two decades, it has become clear that the transport of energy, mass, and magnetic flux in the tail of Earth's magnetosphere often is mediated by fast plasma flows within the plasma sheet, structured in space and time [e.g., *Baumjohann et al.*, 1990; *Angelopoulos et al.*, 1992, 1994; *Petrukovich et al.*, 2001]. These kinds of flows, with velocities upward of 400 km/s, have been termed bursty bulk flows (BBFs) [*Angelopoulos et al.*, 1992].

It is not well known how bursty bulk flows interact with the plasma and magnetic fields on their course to and in the inner magnetosphere. While the acceleration of BBFs has been addressed by considering them as flux tubes of decreased entropy [e.g., *Wolf et al.*, 2009, and references therein], an understanding of the actual forces affecting the flux tube is important. It is clear that BBFs will be affected by both magnetic forces and plasma pressure gradients, but their relative role is unclear. *Shiokawa and Haerendel*, [1997] report that the occurrence frequency of BBFs decreases between 19 and 9 R_E (most likely because of braking of the flow below the threshold of definition) but is still finite at 9 R_E, and similar results are given by *Angelopoulos et al.* [1994] and *Baumjohann et al.* [1990]. (When we discuss acceleration and braking of the BBF plasma in this paper, we refer to the increase or decrease of the bulk plasma flow velocity, perpendicular to the magnetic field.) *Palin et al.* [2012] report on dipolarization fronts (presumably related to BBFs) all the way in to 7 R_E geocentric distance, while *Fu et al.* [2012] report on a rapid decrease of the dipolarization front occurrence rate between 15 and 10 R_E. *Hamrin et al.* [2014], based on energy conversion arguments, show that there is evidence of flow braking between 20 and 15 R_E. In addition, it has been suggested that flows may divert azimuthally [e.g., *Kauristie et al.*, 2003; *Pitkänen et al.*, 2011] or brake in an oscillatory manner [e.g., *Chen and Wolf*, 1999; *Panov*, 2010; *Nakamura et al.*, 2013, 2014] at the entry of the inner magnetosphere.

The magnetic force per unit volume acting on a plasma element can be written as

$$\mathbf{j}\times\mathbf{B} = -\nabla\left(\frac{B^2}{2\mu_0}\right) + \frac{1}{\mu_0}(\mathbf{B}\cdot\nabla)\mathbf{B} = \mathbf{f}_{\mathrm{grad}} + \mathbf{f}_{\mathrm{curv}}, \quad (1)$$

where $\mathbf{f}_{\mathrm{grad}}$ represents the gradient of a magnetic pressure and $\mathbf{f}_{\mathrm{curv}}$ represents a magnetic field tension or curvature force. While the curvature part of the magnetic force is associated with an acceleration of the BBF plasma, some authors attribute the braking in the inner magnetosphere mainly to an increasing magnetic field pressure gradient [*Shiokawa and Haerendel*, 1997; *Nakamura et al.*, 2013]. Others consider

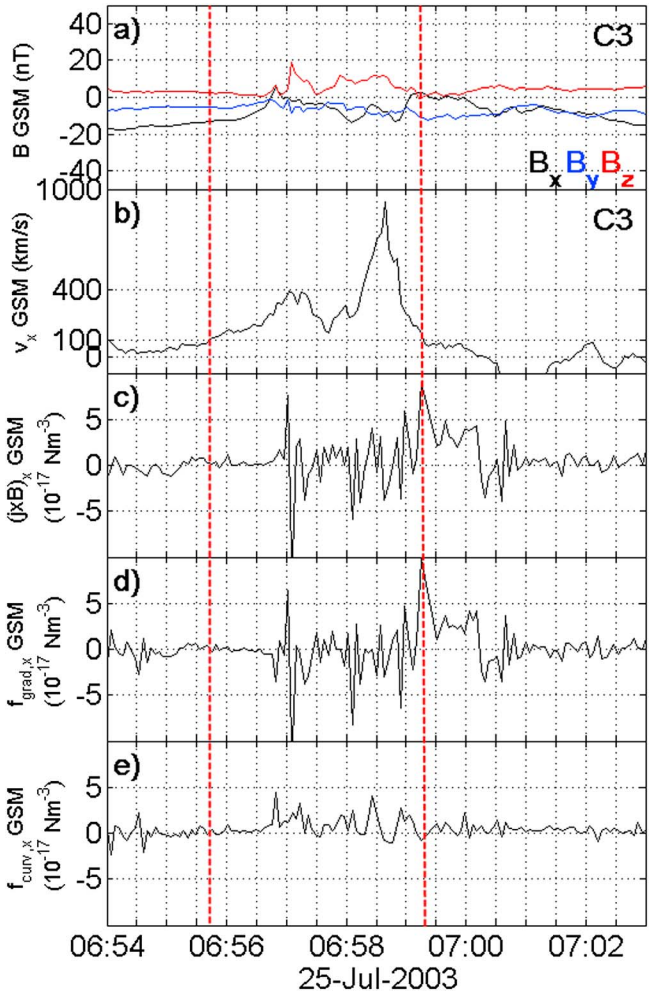

Figure 1. Bursty bulk flow event from 25 July 2003. The panels show from top to bottom the three components of the magnetic field measured by Cluster 1, the *x* component of the ion flow from the HIA instrument and the *x* components of the $\mathbf{j} \times \mathbf{B}$ force density, magnetic pressure gradient force density, and curvature force density. The GSM coordinate system is used for all quantities. The red lines show the beginning and end of the BBF event according to the definition of section 2.2.

the plasma pressure gradient to be equally important [*Ma et al.*, 2009; *Kim et al.*, 2010; *Li et al.*, 2011; *Palin et al.*, 2012] or dominant [*Birn et al.*, 1999]. It is unclear whether the magnetic field pressure gradient is due to the increasing dipole field closer to Earth or to a pileup of magnetic flux in front of the BBF. This pileup, known as a dipolarization front, or magnetic flux pileup is reported to either accelerate or decelerate the BBF plasma, depending on the circumstances [*Hamrin et al.*, 2014; *Li et al.*, 2011].

The uncertainties in how BBFs penetrate into the inner magnetosphere lead to an uncertainty in their role in energy, mass, and magnetic flux transport in that region. The purpose of this paper is to determine the average magnetic forces acting on BBFs as they propagate toward Earth. This is an important part of determining the force balance, which ultimately determines the fate of BBFs in the inner magnetosphere.

2. Method

2.1. Instrumentation

The four Cluster satellites were launched in 2000 in a polar orbit with a perigee of 4.0 R_E geocentric distance and an apogee of 19.8 R_E. We use data from the Cluster Ion Spectrometry (CIS) High Energy Analyzer (HIA) [*Rème et al.*, 2001] for the ion flow velocity (available on spacecraft (S/C) 1 and 3) and the Fluxgate Magnetometer (FGM) [*Balogh et al.*, 2001] for the DC magnetic field. We use spin resolution (4 s) data for both data sets.

2.2. Event Identification

To identify BBF events, we scan Cluster HIA data from the time period of 1 July 2003 to 31 October 2003, using data from S/C 3. During this time, the Cluster apogee is located in the magnetotail, and the spacecraft separations are small, on the order of 100 km. Our criteria for classifying an enhanced magnetospheric flow are similar to what has been used in earlier studies, e.g., by *Angelopoulos et al.* [1994] and *Cao et al.* [2006], and are the following:

1. A BBF event is a time interval where the ion flow velocity in the x_{GSM} direction (v_{ix}) is greater than 100 km/s for all measurement points and where $v_{ix} > 400$ km/s during some time of that interval.
2. We only consider events where the ion flow velocity v_{ix} is either dominatingly in the direction perpendicular to the magnetic field or where the perpendicular and parallel velocities are comparable. Events with a mainly parallel ion velocity are neglected.

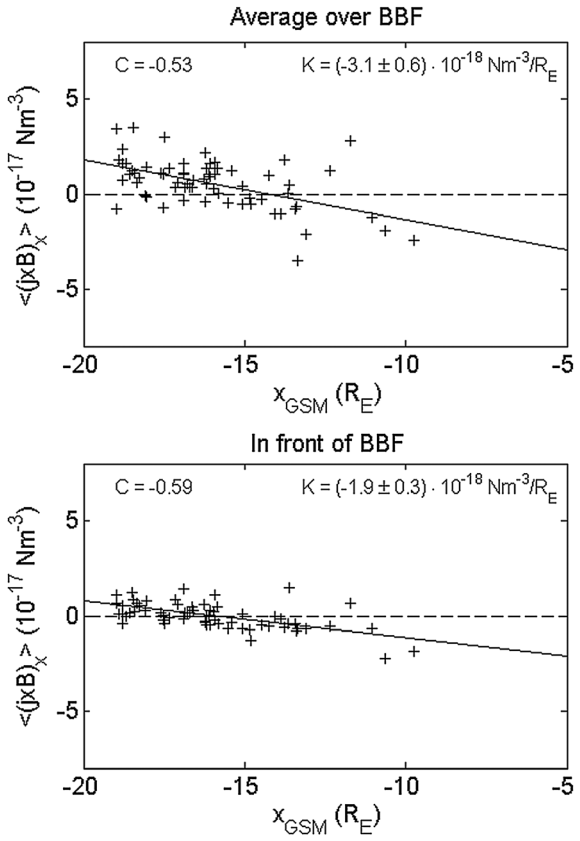

Figure 2. Averages of the x component of $\mathbf{j}\times\mathbf{B}$ (in the GSM coordinate system) for the 67 events of the study, as a function of x_{GSM}. The top plot shows the average over the BBF event, the bottom plot shows the average over 15 min before the BBF event. The correlation coefficients C and the slope K of the resulting linear fit (and the standard error), which is also indicated by the solid line, are shown.

3. If the end of one BBF event is within 30 s of the beginning of another event, the two events are merged and are considered to belong to the same BBF. This is somewhat more restrictive than similar criteria used by other authors [e.g., *Angelopoulos et al.*, 1994; *Cao et al.*, 2006].
4. We further require that $x_{GSM} < 0\ R_E$ and that $\sqrt{x_{GSM}^2 + y_{GSM}^2} > 10\ R_E$.

The events are found by a preliminary automatic scanning of the data and are then manually inspected with regards to criteria 2 and 3 and general quality of the data. It turns out that criterion 2 in practice means that most events are located in the region where $|z_{GSM}| < 4\ R_E$, which means that the selected events are typically located within the central plasma sheet. All events are located in the interval $-15.4 < y_{GSM} < 9.7$, with a majority of them within $|y_{GSM}| < 10\ R_E$.

2.3. Calculation of the j × B Force Density

In order to investigate the $\mathbf{j}\times\mathbf{B}$ force density in a flux tube element associated with a BBF, we calculate the current density $\mathbf{j}$ from the static limit of Ampère's law

$$\mathbf{j} = \frac{1}{\mu_0}\nabla\times\mathbf{B}. \tag{2}$$

The curl is estimated by the reciprocal vector method [*Chanteur*, 1998; *Vogt et al.*, 2008] where the spatial derivatives are approximated by linear interpolation between the vertices of the spacecraft tetrahedron. This method is equivalent to the curlometer method [*Vogt et al.*, 2008] and is valid for current systems with scale sizes larger than the spacecraft separations [*Robert et al.*, 1998; *Dunlop et al.*, 2002].

While calculating $\mathbf{j}$, we have inspected the data for offsets, both in $\mathbf{B}$ and in the calculated current densities, and for a very few cases, we have manually corrected for these. Even in these cases, the final averages of the forces did not change appreciably. We have also calculated the average of both $|\nabla\times\mathbf{B}|$ and $|\nabla\cdot\mathbf{B}|$ over the BBF intervals. A nonzero value of the divergence is an effect of several factors, including nonoptimal spacecraft configuration, the ratio of magnetic field strength to measurement uncertainty, and truncation errors, and indicates a general error level [e.g., *Robert et al.*, 1998]. The calculation of the average divergence shows that it has a rather constant value, less than 50% of the curl, which is considered satisfactory [e.g., *Anekallu et al.*, 2011], for all but one event. However, since it is not close to zero, the errors associated with it will add somewhat to the spread in the data.

After calculating $\mathbf{j}$, the $\mathbf{j}\times\mathbf{B}$ force density is calculated by taking the cross product with the magnetic field vector, averaged over the four spacecraft. (The large-scale magnetic field does not vary much in absolute magnitude between the spacecraft but only in the relatively small variations introduced by the currents floating in the vicinity of the spacecraft.) From the reciprocal vector method, also $\mathbf{f}_{grad}$ and $\mathbf{f}_{curv}$ can be readily estimated [*Chanteur*, 1998; *Vogt et al.*, 2008].

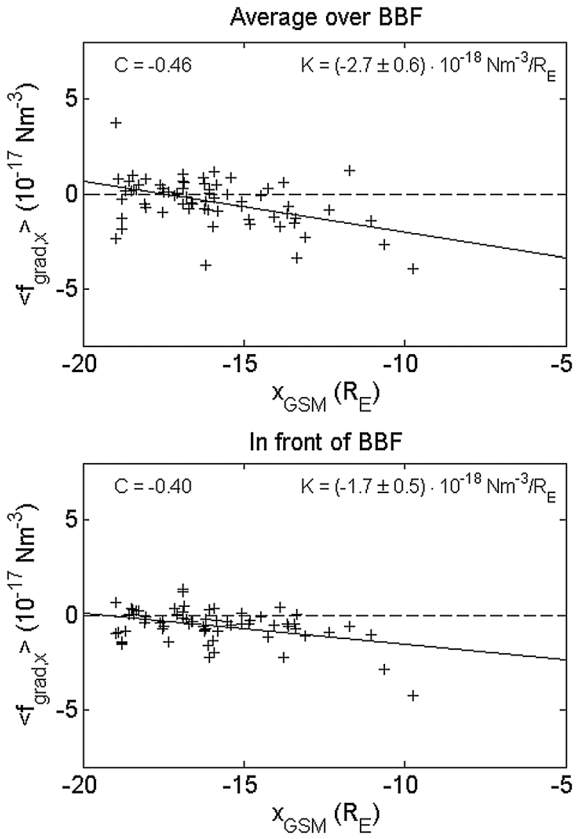

Figure 3. Same as Figure 2 but for the magnetic pressure gradient force $\mathbf{f}_{grad}$.

Figure 1 shows a typical result from the analysis described above, with a BBF event from 25 July 2003, which according to the criteria above starts at 06:55:43 UT and ends at 06:59:21 UT. The Cluster flotilla position in GSM coordinates was (−15.1, −11.9, 0.2) R_E, at the time. As a sanity check, we note that temporal resolution of 4 s corresponds to scale sizes of 4 s times a typical plasma flow velocity of 200 km/s, assuming that the current system associated with the BBF moves together with it, of 800 km. This is appreciably larger than the spacecraft separation, which is on the order of 100 km. We note that the resulting currents are on the order of 10 nA/m^2, which is consistent with the results reported by *Forsyth et al.* [2008]. The x component of the $\mathbf{j}\times\mathbf{B}$ force density exhibits considerable small-scale variation but shows a consistent behavior; in that, the curvature force is mainly positive during the main part of the event, whereas the gradient force is generally negative (considering only the x components). For this particular event, the curvature force generally dominates the gradient force, resulting in a positive average $\mathbf{j}\times\mathbf{B}$ force in the x direction, accelerating the BBF plasma toward Earth.

In order to study statistically the mean force acting on BBF plasma regions, we calculate the mean value of $(\mathbf{j}\times\mathbf{B})_x$, $f_{grad,x}$, and $f_{curv,x}$ over the whole BBF event. For the event in Figure 1, the resulting averages were $<(\mathbf{j}\times\mathbf{B})_x> = 4.4\cdot10^{-18}\,\mathrm{Nm}^{-3}$, $<f_{grad,x}> = -3.9\cdot10^{-18}\,\mathrm{Nm}^{-3}$, and $<f_{curv,x}> = 8.3\cdot10^{-18}\,\mathrm{Nm}^{-3}$, where the brackets indicate averaging between the start and end times of the event. These orders of magnitudes are consistent with the result of a case study by *Li et al.* [2011], based on a magnetic field fit to spacecraft observations. In order to test the robustness of our results, we also calculate averages over parts of the BBF event, e.g., the front half, defined as all data points measured before the maximum of v_{ix}, and the back half, defined analogously. The results reported on below do not change qualitatively when we use different methods of calculating the averages. For comparison, we also want to calculate the average forces on the plasma for non-BBF times. We do this by averaging over a time of 15 min before the start of the BBF event, except when this time contains another BBF event. The resulting average will then typically show the average magnetic forces on the plasma in front of the BBF.

3. Statistical Results

Our search resulted in 67 BBF events fulfilling the criteria of section 2.2. We will focus on the x direction, which (on the average) is the dominant direction of earthward fast flows [*Juusola et al.*, 2011], and the direction in which the magnetic force is expected to be the most important one when considering the BBF dynamics. However, we have studied the y component of the forces as well but have found no systematic dependence on position, and we do not show these data here.

In Figure 2 (top), we plot the average $<(\mathbf{j}\times\mathbf{B})_x>$ for all events as a function of x_{GSM}, and in Figure 2 (bottom), we present the corresponding average in front of the BBF event. Figures 3 and 4 show results for $<f_{grad,x}>$ and

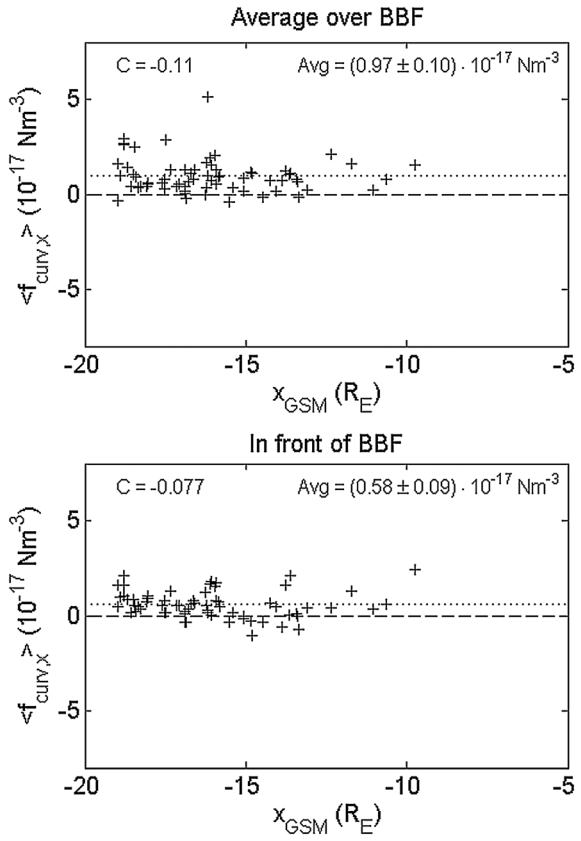

Figure 4. Same as Figure 2 but for the curvature force $\mathbf{f}_{curv}$. Instead of a linear fit, indicated is the average over all data points, both as the value *Avg* and as the dotted line.

$<f_{curv,x}>$ in a similar format. For each of the panels, a simple linear regression is performed, and the correlation coefficient is calculated. The resulting correlation coefficients are displayed in each plot, together with their standard error, and the result of the linear model is plotted. (Except for Figure 4, where a very low correlation coefficient is found. Here is instead indicated the average value of $<f_{curv,x}>$ for each panel.)

4. Discussion

There is some spread in the data presented in Figures 2–4, but a consistent picture emerges. Figure 4 shows that the curvature force density is generally positive for BBF events, acting to accelerate the plasma earthward. This is consistent with magnetic field lines being stretched during a substorm growth phase or similar conditions and subsequently being severed by an onset of localized reconnection [e.g., *Sergeev*, 2005: *Birn et al.*, 2011], resulting in an acceleration of the plasma as the field line relaxes toward a more dipole-like configuration.

Before/in front of the BBF event, the curvature force is still positive and nonzero but appreciably smaller than for the BBFs. We interpret this as the magnetic force applied by magnetic field lines associated with the more gentle Dungey cycle flow associated with non-BBF times [*Dungey*, 1961]. The fact that the curvature force density associated with BBFs remains relatively constant with x_{GSM} may be an indication that any decrease of the curvature of the field lines associated with the BBF is compensated by an increasing magnetic field strength closer to Earth. This increase may be due to an increasing pileup of frozen-in magnetic field lines in front of and inside the BBF in the form of a dipolarization front [e.g., *Nakamura et al.*, 2002; *Li et al.*, 2011; *Fu et al.*, 2012; *Hamrin et al.*, 2014]. Such a magnetic field pileup may act to increase the magnitudes of both $\mathbf{f}_{curv}$ and $\mathbf{f}_{grad}$, as evidenced by equation (1). An alternative interpretation is that this is a selection effect; in that, only BBFs with a sufficient curvature force will be able to make it to the near-Earth tail where we observe them.

The magnetic pressure gradient force density (see Figure 3) is small at great distances from Earth and gradually becomes more negative closer to Earth. This is again true for both BBF events and non-BBF times, but the force density changes more rapidly for the BBF events. We can interpret this as a magnetic field pressure gradient associated with the increasing magnitude of the dipole magnetic field as we move closer toward the Earth, with an additional magnetic pressure gradient being present for the BBF events. This is again likely associated with magnetic flux pileup regions, as discussed above. In this case, the increasing magnetic field associated with these will tend to brake the flow [*Birn et al.*, 2011; *Fu et al.*, 2012; *Hamrin et al.*, 2014].

The combined magnetic force of curvature and magnetic pressure gradient acting on the BBF plasma is seen in Figure 2 to be typically positive for larger distances. At a certain distance from Earth, it changes sign. Taking into consideration the uncertainties in the regression analysis, this happens at $x_{GSM} = 13.9 \pm 0.6\ R_E$, after which it acts to brake the BBF plasma. We can therefore conclude that this distance represents the minimum distance from Earth at which the BBF plasma will begin to decelerate.

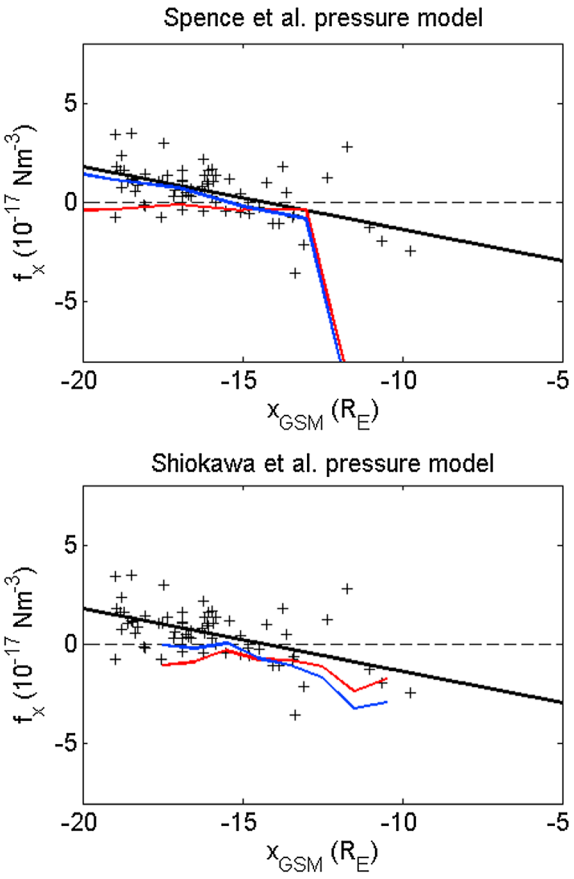

Figure 5. The values for the average x component of $\mathbf{j}\times\mathbf{B}$ for the 67 events (crosses), and the corresponding linear fit (black line), as well as the estimated values of the plasma thermal pressure gradient, obtained from (top) *Spence et al.* [1989] and from (bottom) *Shiokawa and Haerendel* [1997], as the red line, as well as the sum of the magnetic force (using the fitted trend line) and the plasma pressure gradient (blue line), as a function of x_{GSM}.

The other main force acting on that plasma is the thermal plasma pressure gradient. The balance between the magnetic force and the thermal pressure force determines how far in toward Earth the BBF will travel, and the additional force of the thermal pressure gradient will move the position of zero total force farther away from Earth. Unfortunately, it is difficult or impossible to determine the plasma pressure gradient from Cluster data due to too large uncertainties in the interspacecraft calibrations [*Hamrin et al.*, 2013].

We can, however, use statistical measurements of the plasma pressure as a function of distance to Earth to estimate the typical values of the plasma pressure gradient in order to compare it with the magnetic force. We use the results from the studies by *Spence et al.* [1989] and *Shiokawa and Haerendel* [1997], which provide statistical plasma pressure profiles in the equatorial plane. In Figure 5, we again show the x component of the $\mathbf{j}\times\mathbf{B}$ force density, together with the fitted trend line. The estimated value of the plasma thermal pressure gradient (red line), obtained from Figure 8 by *Spence et al.* [1989] (for $K_p^* = 3^-$) in our Figure 5 (top) and from Figure 2 by *Shiokawa and Haerendel* [1997] in our Figure 5 (bottom), is also shown. Finally, the sum of the fitted total magnetic force and the plasma pressure gradient is indicated by the blue line. It can be seen from both estimates that the point at which the plasma begins to decelerate is located somewhat farther away from Earth than where the magnetic force changes sign, at approximately $x_{GSM} = -16.1 \pm 1.8\ R_E$. The uncertainties arise from uncertainties in the regression analysis and differences in the two plasma pressure models used. This result is, in general, consistent with earlier results discussed in the Introduction. However, the flow braking taking place already within 20 R_E reported by *Hamrin et al.* [2014], for BBFs with their velocity peak behind the dipolarization front, may indicate that the plasma pressure gradient obtained from statistical results is underestimated and that localized plasma pressure enhancements in front of the BBFs will act to further brake the flow, as reported by *Liu et al.* [2013].

When the total force profile is known, integration will tell us how far into the magnetosphere the BBF will penetrate. As an example, using the force density profile resulting from the pressure profile of *Spence et al.* [1989], elementary calculation shows that a plasma element of a proton plasma with a number density of 1 cm^{-3} and an initial velocity of 800 km/s at $x_{GSM} = -17\ R_E$, km/s will brake to zero velocity at $x_{GSM} = -11.8\ R_E$. Using the *Shiokawa and Haerendel*'s [1997] results, the plasma would still have a velocity of close to 300 km/s at that point and would penetrate further in toward Earth than $x_{GSM} = -10\ R_E$. This simple example illustrates that a better determination of the local plasma pressure gradient is needed to make a realistic determination of the depth of the BBF penetration. The upcoming Magnetospheric Multiscale mission [*Sharma and Curtis*, 2005] may provide this opportunity.

Acknowledgments
We thank the CIS and FGM teams and the Cluster Active Archive for providing the data. We are grateful to colleagues at the Institute for Space Physics, Uppsala, for providing the IRFU-MATLAB package. Finally, we acknowledge the Swedish National Space Board grants 78/11A-B.

The Editor thanks Kazuo Shiokawa and an anonymous reviewer for their assistance in evaluating this paper.

References

Anekallu, C. R., M. Palmroth, T. I. Pulkkinen, S. E. Haaland, E. Lucek, and I. Dandouras (2011), Energy conversion at the Earth's magnetopause using single and multispacecraft methods, *J. Geophys. Res.*, *116*, A11204, doi:10.1029/2011JA016783.

Angelopoulos, V., W. Baumjohann, C. F. Kennel, F. V. Koroniti, M. G. Kivelson, R. Pellat, R. J. Walker, H. Lühr, and G. Paschman (1992), Bursty bulk flows in the inner central plasma sheet, *J. Geophys. Res.*, *97*(A4), 4027–4039, doi:10.1029/91JA02701.

Angelopoulos, V., C. F. Kennel, F. V. Coroniti, R. Pellat, M. G. Kivelson, R. J. Walker, C. T. Russell, W. Baumjohan, W. C. Feldman, and J. T. Gosling (1994), Statistical characteristics of bursty bulk flow events, *J. Geophys. Res.*, *99*(A11), 21,257–21,280, doi:10.1029/94JA01263.

Balogh, A., et al. (2001), The Cluster magnetic field investigation: Overview of in-flight performance and initial results, *Ann. Geophys.*, *19*, 1207.

Baumjohann, W., G. Paschmann, and H. Lühr (1990), Characteristics of high-speed ion flows in the plasma sheet, *J. Geophys. Res.*, *95*(A4), 3801–3809, doi:10.1029/JA095iA04p03801.

Birn, J., M. Hesse, G. Harendel, W. Baumjohann, and K. Shiokawa (1999), Flow braking and the substorm current wedge, *J. Geophys. Res.*, *104*(A9), 19,895–19,903, doi:10.1029/1999JA900173.

Birn, J., R. Nakamura, E. V. Panov, and M. Hesse (2011), Bursty bulk flows and dipolarization in MHD simulations of magnetotail reconnection, *J. Geophys. Res.*, *116*, A01210, doi:10.1029/2010JA016083.

Cao, J. B., et al. (2006), Joint observations by Cluster satellites of bursty bulk flows in the magnetotail, *J. Geophys. Res.*, *111*, A04206, doi:10.1029/2005JA011322.

Chanteur, G. (1998), Spatial interpolation for four spacecraft: Theory, in *Analysis Methods for Multi-Spacecraft Data*, edited by G. Paschmann and P. W. Daly, pp. 395–418, ESA, Noordwijk.

Chen, C. X., and R. A. Wolf (1999), Theory of thin filament motion in Earth's magnetotail and its application to bursty bulk flows, *J. Geophys. Res.*, *104*, 14,613–14,626, doi:10.1029/1999JA900005.

Dungey, J. W. (1961), Interplanetary field and the auroral zones, *Phys. Rev. Lett.*, *6*, 47–48.

Dunlop, M. W., A. Balogh, K.-H. Glassmeier, and P. Robert (2002), Four-point Cluster application of magnetic field analysis tools: The curlometer, *J. Geophys. Res.*, *107*(A11), 1384, doi:10.1029/2001JA005088.

Forsyth, C., et al. (2008), Observed tail current systems associated with bursty bulk flows and auroral streamers during a period of multiple substorms, *Ann. Geophys.*, *26*(1), 167–184.

Fu, H. S., Y. V. Khotyaintsev, A. Vaivads, M. Andre, and S. Y. Huang (2012), Occurrence rate of earthward-propagating dipolarization fronts, *Geophys. Res. Lett.*, *39*, L10101, doi:10.1029/2012GL051784.

Hamrin, M., P. Norqvist, T. Carlson, and H. Nilsson (2013), The evolution of flux pileup regions in the plasma sheet: Cluster observations, *J. Geophys. Res. Space Physics*, *118*, 6279–6290, doi:10.1002/jgra.50603.

Hamrin, M., et al. (2014), Evidence for the braking of flow bursts as they propagate toward the Earth, *J. Geophys. Res. Space Physics*, *119*, 9004–9018, doi:10.1002/2014JA020285.

Juusola, L., N. Ostgaard, and E. Tanskanen (2011), Statistics of plasma sheet convection, *J. Geophys. Res.*, *116*, A08201, doi:10.1029/2011JA016479.

Kauristie, K., V. Sergeev, O. Amm, M. Kabyshkina, J. Jussila, and E. Donovan (2003), Bursty bulk flow intrusion to the inner plasma sheet as inferred from auroral observations, *J. Geophys. Res.*, *108*(A1), 1040, doi:10.1029/2002JA009371.

Kim, H.-. S., D.-. Y. Lee, S.-. I. Ohtani, E.-. S. Lee, and B.-. H. Ahn (2010), Some statistical properties of flow bursts in the magnetotail, *J. Geophys. Res.*, *115*, A12229, doi:10.1029/2009JA015173.

Li, S.-. S., V. Angelopoulos, A. Runov, X.-. Z. Zhou, J. McFadden, D. Larson, J. Bonnell, and U. Auster (2011), On the force balance around dipolarization fronts within bursty bulk flows, *J. Geophys. Res.*, *116*, A00I35, doi:10.1029/2010JA015884.

Liu, J., V. Angelopoulos, X.-Z. Zhou, A. Runov, and Z. H. Yao (2013), On the role of pressure and flow perturbations around dipolarizing flux bundles, *J. Geophys. Res. Space Physics*, *118*, 7104–7118, doi:10.1002/2013JA019256.

Ma, Y. D., J. B. Cao, R. Nakamura, T. L. Zhang, H. Reme, I. Dandouras, E. Lucek, and M. Dunlop (2009), Statistical analysis of earthward flow bursts in the inner plasma sheet during substorms, *J. Geophys. Res.*, *114*, A07215, doi:10.1029/2009JA014275.

Nakamura, R., et al. (2002), Motion of the dipolarization front during a flow burst event observed by Cluster, *Geophys. Res. Lett.*, *29*(20), 3–1, doi:10.1029/2002GL015763.

Nakamura, R., et al. (2013), Flow bouncing and electron injection observed by Cluster, *J. Geophys. Res. Space Physics*, *118*, 2055–2072, doi:10.1002/jgra.50134.

Nakamura, R., et al. (2014), Low-altitude electron acceleration due to multiple flow bursts in the magnetotail, *Geophys. Res. Lett.*, *41*, 777–784, doi:10.1002/2013GL058982.

Palin, L., C. Jacquey, J.-A. Sauvaud, B. Lavraud, E. Budnik, V. Angelopoulus, U. Auster, J. P. McFadden, and D. Larson (2012), Statistical analysis of dipolarizations using spacecraft closely separated along *Z* in the near-Earth magnetotail, *J. Geophys. Res.*, *117*, A09215, doi:10.1029/2012JA017532.

Panov, E. V., et al. (2010), Plasma sheet thickness during a bursty bulk flow reversal, *J. Geophys. Res.*, *115*, A05213, doi:10.1029/2009JA014743.

Petrukovich, A. A., W. Baumjohann, R. Nakamura, R. Schödel, and T. Mukai (2001), Are earthward bursty bulk flows convective or field-aligned?, *J. Geophys. Res.*, *106*(A10), 21,211–21,215, doi:10.1029/2001JA900019.

Pitkänen, T., A. T. Aikio, O. Amm, K. Kauristie, H. Nilsson, and K. U. Kaila (2011), EISCAT-Cluster observations of quiet-time near-Earth magnetotail fast flows and their signatures in the ionosphere, *Ann. Geophys.*, *29*, 299–319, doi:10.5194/angeo-29-299-2011.

Rème, H., et al. (2001), First multispacecraft ion measurements in and near the Earth's magnetosphere with the identical Cluster Ion Spectrometry (CIS) experiment, *Ann. Geophys.*, *19*, 1303.

Robert, P., M. W. Dunlop, A. Roux, and G. Chanteur (1998), Accuracy of current density determination, in analysis methods for multispacecraft data, ISSI Sci. Rep., SR-001, Kluwer Acad., Norwell, Mass.

Sergeev, V. A. (2005), Bursty bulk flows and their ionospheric footprints, in *Multiscale Processes in the Earth's Magnetosphere: From Interball to Cluster*, pp. 289–306, Springer, Netherlands.

Sharma, A. S., and S. A. Curtis (2005), Magnetospheric multiscale mission, in *Nonequilibrium Phenomena in Plasmas*, pp. 179–195, Springer, Netherlands.

Shiokawa, K., and G. Haerendel (1997), Breaking of high-speed flows in the near-Earth tail, *Geophys. Res. Lett.*, *24*, 1179–1182, doi:10.1029/97GL01062.

Spence, H. E., M. G. Kivelson, R. J. Walker, and D. J. McComas (1989), Magnetospheric plasma pressures in the midnight meridian: Observations from 2.5 to 35 R_E, *J. Geophys. Res.*, *94*(A5), 5264–5272, doi:10.1029/JA094iA05p05264.

Vogt, J., G. Paschmann, and G. Chanteur (2008), Reciprocal vectors ISSI SR-008, pp. 33–46 .

Wolf, R. A., Y. Wan, X. Xing, J.-C. Zhang, and S. Sazykin (2009), Entropy and plasma sheet transport, *J. Geophys. Res.*, *114*, A00D05, doi:10.1029/2009JA014044.